Nonlinear Model Identification of a Shock Absorber Dynamics

Fadly Jashi Darsivan*, Mohd Helmi Hamid[+], Mohamad Fahmi Abdullah[+]

* Assistant Professor, Faculty of Engineering, International Islamic University Malaysia, Jalan Gombak, 53100, Kuala Lumpur, Malaysia.

[+] Final Year Undergraduate Students, Faculty of Engineering, International Islamic University Malaysia, Jalan Gombak, 53100, Kuala Lumpur, Malaysia.

***Abstract*—**The paper discusses on the technique of modeling a nonlinear dynamics of a commercially available automotive shock absorber. The damper was tested on the damper test bench to obtain its dynamic characteristics. The characteristics include the force-displacement and the force-velocity diagrams. From the result obtained experimentally it clearly showed that the automotive damper behaves nonlinearly. The plot also indicates the hysteresis of the damper at different frequency levels. From the force-velocity graphs a backbone model was then developed and plot. Based on this graph three types of non-parametric model namely the linear model, polynomial model and the power model were then obtained through curve fitting method. The models were then verified by using another set of experimentally obtained data. Based on these models quarter car simulations were conducted. From the simulation it was clear that the linear model showed a large difference in terms of vertical displacement of the sprung mass at the natural frequency compared to the polynomial and the power models.

***Keywords*—**Damper, hysteresis, backbone, polynomial model, power model.

I. INTRODUCTION

The shock absorber or damper is one of the automotive components that behaves nonlinearly (Rao, Grueberg and Torab, 1999; Duym, Steins and Reybrouck, 1997). Thus, it would not be correct or adequate to assume that the damping coefficient of the shock absorber to have a single value describing its behavior at different levels of frequencies and speed (Dixon, 2007; Lee, 2007). The paper discusses the technique of obtaining a non-parametric nonlinear model of the damper that was extracted from an experiment. The mathematical model is defined nonparametric since the coefficients of the equations do not actually represent any physical meaning of the damper. However, this model would be suitable to be used in the quarter car model to simulate its ride performances. The damper was used for a Honda Civic vehicle and was tested using an MTS 850 damper testing system that was available at PROTON Bhd. From the experiment the damper

characteristic curve was obtained. From this curve the hard point i.e. the maximum values of the force at the maximum velocities were then extracted. These hard point data were plot and the plot is known as the backbone model of the damper.

In this paper three different models were obtained. The first was the linear model, secondly the polynomial of the order of four and finally the power model. In order to validate the empirical models a time history of the damping force data were collected through experiment. These data represent the damping force at a constant frequency level and at a constant damping stroke for finite period of time. The response of the sprung mass displacement and acceleration using each of the models was obtained through a quarter car model simulation using Scilab open source software. The purpose of the simulation was to compare the responses of the sprung mass when the car traveled on a predefined road profile.

The rest of the paper is organized in the following manner. The next heading will be discussing on the characteristic of a typical automotive damper and the experimental procedure and setup to obtain this characteristic. Next, the paper discusses the backbone model and how this model is obtained. Then, the next topic is a brief description of the algorithm to obtain the empirical model and the three models are then defined and presented. Then for validation purpose the time history of the damping force for each model are compared with the data obtained from experiment and illustrated by a time history plot. Once the force history comparison is done the quarter car ride performance simulation will be presented. Finally, the paper closes the topic with discussions and conclusions.

II. Damper Characteristic And Experimental Procedure

A typical shock absorber would have the following characteristics depicted in fadlyimage1a.jpg and fadlyimage1b.jpg.

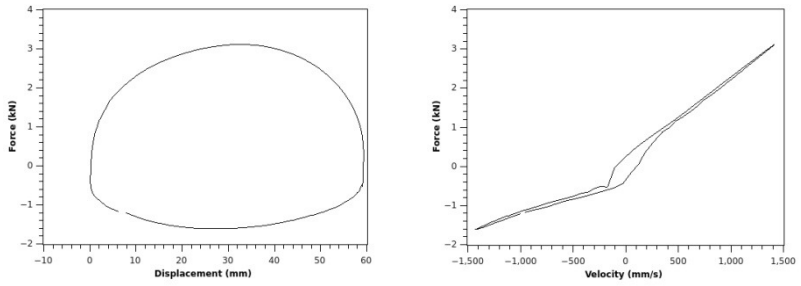

(a) (b)

Fig. 1 The characteristic of a typical damper (a) Force-Displacement graph

(b) Force-Velocity graph

fadlyimage1a.jpg and fadlyimage1b.jpg are the damping characteristic of a shock absorber at a frequency of 8 Hz and a peak-to-peak stroke of 60 mm taken in one cycle of the experiment. fadlyimage1a.jpg depicts the two region of the damper i.e. the positive force region is known as the rebound (moving up) region and the negative force region is the compression (moving down) region (Kasteel, et al. 2007). From the figure it shows that the damping force magnitudes between rebound and compression are different. To be more precise the rebound damping force is much higher compared to the compression region (Gillespie, 1992). fadlyimage1a.jpg depicts the force velocity characteristics of the damper. A similar pattern can also be observed i.e. rebound force is larger than compression force. Another interesting observation is also the hysteresis effect of the damper i.e. damping force of the shock absorber do not follow the same path as it moves from the rebound region to the compression region (Surace, Worden, Tomlinson, 1992). This phenomenon is caused by the construction of the damper piston assembly where it consists of a main piston body and a stack of shims that restricts the motion of fluid as the damper moves up and down (Ferdek and Luczko, 2012).

To capture the characteristics of the damper at different frequency levels a front shock absorber of a Honda Civic was tested using the MTS 850 damper testing machine. The damper was subjected to a constant stroke distance of 60 mm (30 mm rebound and 30 mm compression) at different levels of frequency i.e. 0.3 Hz, 1 Hz, 3 Hz, 5 Hz and 8 Hz. The frequency variation is essential to capture a broad range of the damper characteristic. This method was also used by Subramaniam, Surampudi and Thomson (2003) where they have subjected a shock absorber to a pure sine wave on an MTS machine with a peak-to-peak displacement amplitude of 2mm.

Fadlyimage2(a)(b)(c)(d)(e).jpg shows the result of the experiment conducted. From the figure it can be clearly observed that as the frequency increases the damping force also increases as well as the hysteresis area. It is also observed that the damping coefficient, *c*, changes as the frequency is increased by noticing the gradient of the Force-Velocity graphs conforming that the shock absorber behaves nonlinearly.

III. Damper Backbone Model

The backbone model of the damper is basically the hard points of the Force-Velocity diagram (Dzierżek, Knapczyk and Maniowski, 2008). Hard points are the pinnacle values of the damping force for each frequency level. These pinnacle values also include the magnitude of the damping force in the compression region. Based on this then the backbone model of the damper can be depicted as in fadlyimage3.jpg.

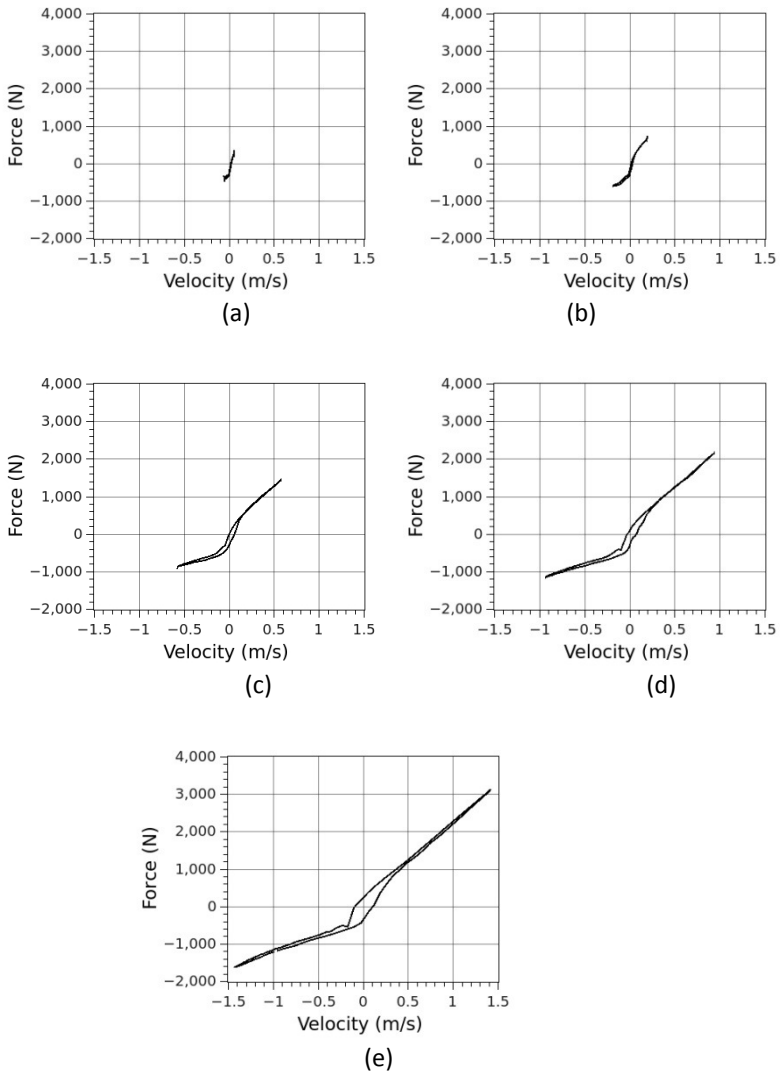

Fig. 2 The damping velocity characteristics of the shock absorber subjected to a constant stroke at different frequency level (a) 0.3 Hz, (b) 1 Hz, (c) 3 Hz, (d) 5 Hz and (e) 8 Hz.

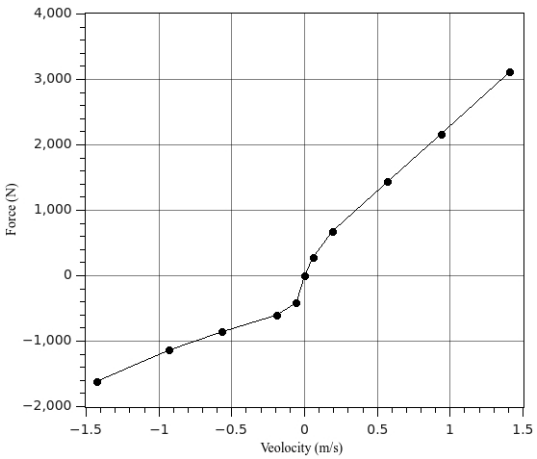

Fig. 3 Backbone model of the damper

From the figure in the rebound region it can now be clearly seen that the damper will eventually decreases its damping coefficient value, *c*, as the speed of the damper increases. It can also be observed that the maximum magnitude force in rebound region is relatively much larger compared to the magnitude in the compression region. From the backbone model the magnitude of the damping force during rebound is approximately more than 3000 N while the force during compression is less than 2000 N. This is consistent with the intention that when the car is travelling on a bump the shock absorber will be compressed and the damping force should be small as to reduce the force that pushes the body thus reducing the motion of the sprung mass. While the car is travelling through a pot hole the damping is preferably large so as to maintain a good road holding so that the displacement of the sprung mass will be ideally remain constant through out the travel period (Gillespie,1992).

Taking the gradient of the damper in the rebound region by differentiating the Force-Velocity diagram will give the result in fadlyimage4.jpg.

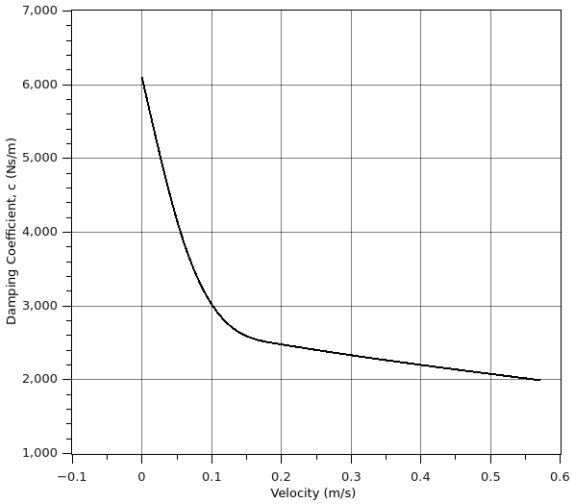

Fig. 4 The damping coefficient of the damper in the rebound region

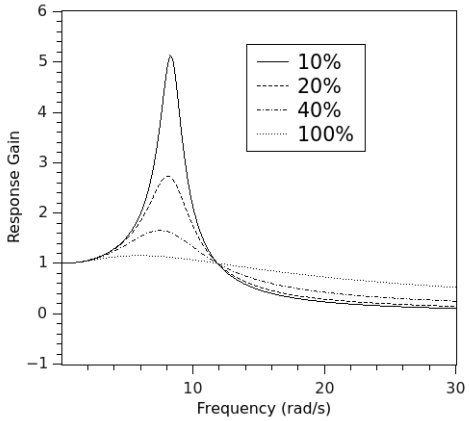

Fig. 5 Effect of damping at different suspension damping coefficient

Fadlyimage4.jpg illustrates how the gradient of the Force-Velocity diagram i.e. the damping coefficient reduces sharply between the velocity of 0 to 0.1 m/s and reduces gradually as the speed of the damper further increases. Fadlyimage5.jpg could help explain these desired characteristics. At the resonance frequency increased in damping coefficient decreases the response gain i.e. the acceleration of the sprung mass reduces thus, improving the ride quality of the vehicle. However, at this level of damping coefficient the isolation of the body from the vertical road disturbance is

deteriorating at frequency above resonance. At the same time if the damping coefficient is decreased it causes large body motion at the resonance frequency but better isolation above this region. Therefore, it can be concluded to achieve better isolation in the resonance frequency the damping coefficient has to be large but at the frequency above resonance damping coefficient has to be reduced. This is the conflicting characteristic of a shock absorber that automotive engineers have to compromise in its design.

IV. Empirical Model of the Damper

Based on fadlyimage3.jpg three empirical models of the damping force were developed namely the linear model, 4th order polynomial and finally the power model. The polynomial model and power model will also be referred as the nonlinear models. These models are in the following forms:-

$$F_d = a\dot{x} \quad \text{(linear model)} \tag{1}$$

$$F_d = \sum_{i=0}^{4} c_i \dot{x}^i \quad (4^{\text{th}} \text{ order polynomial model}) \tag{2}$$

$$F_d = d\dot{x}^e \quad \text{(power model)} \tag{3}$$

Where *a* and *b* are the coefficients of the linear model, c_i is the coefficient of the polynomial model and *d* and *e* are the coefficients of the power model and $\dot{x}$ is the velocity. These models are considered as non-parametric since all the coefficients related to each of the model do not represent any physical interpretations of the shock absorber. However, the advantage of having these models they could easily be used for the purpose of simulating the ride dynamics of a vehicle.

Levenberg-Marquardt algorithm was applied as the curve fitting method. 10000 iterations and a tolerance of 0.0001 were used. Once the iterations were completed the parameters were obtained as tabulated in fadlytable1.xlsx. fadlytable2.xlsx illustrates the root mean squared (RMS) error for each of the model at different region i.e. rebound and compression regions. From the values of the RMS error it can be observed that the linear model is less accurate compared to the experimental data while, the polynomial and the power models showed a better level of accuracy.

TABLE 1

Parameter Values for 3 Different Damper Models

Symbol	Value
a	2.2870e+03; $\dot{x} > 0$ (rebound)
	1.2205e+03; $\dot{x} < 0$ (compression)
c_1	4801.47; $\dot{x} > 0$ (rebound)
	5706.53; $\dot{x} < 0$ (compression)
c_2	-7379.01; $\dot{x} > 0$ (rebound)
	14035.81; $\dot{x} < 0$ (compression)
c_3	7245.29; $\dot{x} > 0$ (rebound)
	14260.31; $\dot{x} < 0$ (compression)
c_4	2351.50; $\dot{x} > 0$ (rebound)
	4675.81; $\dot{x} < 0$ (compression)
d	2.3330e+03; $\dot{x} > 0$ (rebound)
	1.2683e+3; $\dot{x} < 0$ (compression)
e	0.8; $\dot{x} > 0$ (rebound)
	0.4; $\dot{x} < 0$ (compression)

TABLE 2

Root Mean Squared Error for Various Models

No.	**Model**	**Region**	**RMS Error**
1	Linear	Rebound	148.94
		Compression	242.98
2	Polynomial	Rebound	23.26
		Compression	104.81
3	Power	Rebound	64.36
		Compression	98.55

Fadlyimage6.jpg depicts the force history of the various models compared to the data obtain through experiment. In the figure the experimental data was obtained by applying a peak-to-peak amplitude of 60mm at a frequency of 7 Hz. From the figure the models could represent more accurately in the rebound region compared to the compression

region. This is also consistent with the value of the RMS error where the error is relatively larger at the compression region. It can also be seen that the linear model has a larger magnitude at the crest and trough compared to the nonlinear models.

V. Quarter Car Simulation

To observe the response of the sprung mass for each of the damper model a quarter car simulation shown in Fadlyimage7.jpg was conducted. Two types of road profile input were considered i.e. a step road profile and a sine wave. The step road profile was used in order to observe the transient response of the sprung mass and to investigate the settling time of the mass. While the sine wave was implemented to investigate the steady state response of the mass while the system was excited at the natural frequency of the body. The road profiles used in the simulation can be illustrated as in fadlyimage8a.jpg and fadlyimage8b.jpg. The data in fadlytable3.xlsx were used as the parameters for the quarter car model.

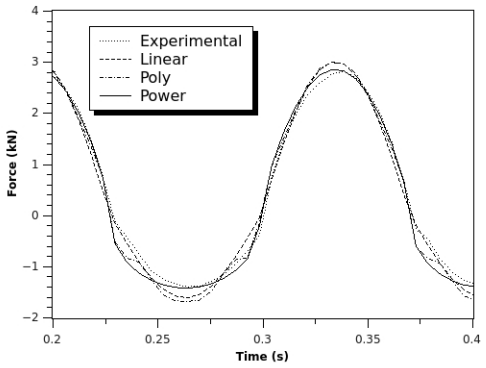

Fig. 6 Time history of damping force comparison for different damper model

The equation of motion for the quarter car model can be defined as:-

$$m_s\ddot{x}_s(t) + F_d(\dot{x}) + k_s x_1 = 0 \quad (4)$$

$$m_{us}\ddot{x}_{us} + k_{us}x_{us} - F_d(\dot{x}) - k_s x_1 = k_{us}x_r \quad (5)$$

Where,

$\dot{x} = (\dot{x}_s - \dot{x}_{us})$

$x_1 = (x_s - x_{us})$

Based on equation (6) and from the quarter car model parameters it can be calculated that the natural frequency of the sprung mass is 1.28 Hz which

is typical for a passenger car.

$$f = 0.159\sqrt{\frac{(k_{us} \times k_s)/(k_{us}+k_s)}{m_{us}}} \quad (6)$$

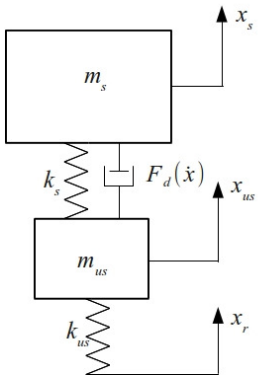

Fig. 7 Quarter car model

When subjected to a step road disturbance with a magnitude of 0.03 m downward the results of the sprung mass displacement can be illustrated as in fadlyimage9a.jpg. From the figure it can be seen that the linear damper model has a large overshoot of approximately -0.02 m whereas, the polynomial and the power model have overshoot values of approximately -0.0077 m and -0.0052 m respectively. Another important observation that can be seen from the graph is the settling time that varies from one model to another. The linear model has the largest settling time i.e. approximately 1.5 seconds and the nonlinear model showed a similar trend of having faster settling time of less than a second.

Table 3

Quarter Car Model Parameters

Symbol	Description	Value	Unit
m_s	Sprung mass	291	kg
m_{us}	Unsprung mass	17.5	kg
k_s	Suspension stiffness	20500	N/m
F_d	Damping force model		N
k_{us}	Tyre stiffness	232000	N/m

$x_s(t)$	Spung mass displacement	m
$x_{us}(t)$	Unsprung mass displacement	m
$x_r(t)$	Road profile	m

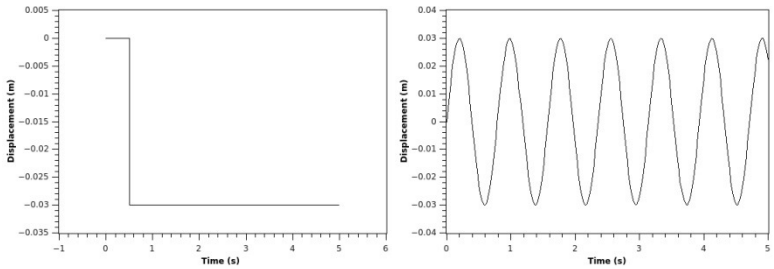

(a) (b)

Fig. 8 The road profile for the quarter car simulation

VI. RESULTS

Fadlyimage9b.jpg shows the acceleration response of the sprung when subjected to the same road disturbance. From the figure it can be seen that both the linear model and the power have large acceleration magnitudes compared to the polynomial model. The linear model and power model have accelerations magnitudes of approximately 14 m/s^2 whereas the polynomial model has an acceleration magnitude of approximately 5 m/s^2. However, the settling time for the linear model is noticed to be longer compared to both the polynomial and power model. Having faster settling time improves the ride quality of the vehicle and reduces the discomfort level of the passenger (Zhu, Khajepour and Esmailzadeh, 2012; Ihsan, et. al, 2009).

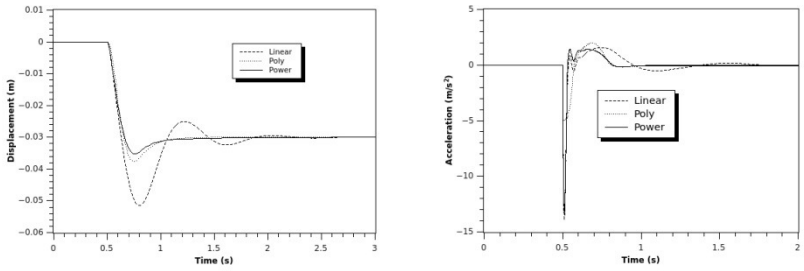

(a) (b)

Fig. 9 Response of the sprung mass subjected to a step road disturbance (a) displacement and (b) acceleration

Fadlyimage10a.jpg depicts the sprung mass steady state displacement response when the quarter car was subjected to a sine wave. The disturbance has a magnitude of 0.03 m and a frequency of 1.27 Hz which is the same as the natural frequency of the body.

The linear model has a peak-to-peak amplitude of 0.0968 m while the polynomial model and the power model have peak-to-peak amplitudes of 0.0783 m and 0.0758 m respectively. This difference is expected since the RMS error for all the damper models varied with linear model being the least accurate. It can also be observed that the crest and the trough magnitudes for all the models showed different values. The reason for this is because of the different model coefficients at the rebound and compression region of the damper.

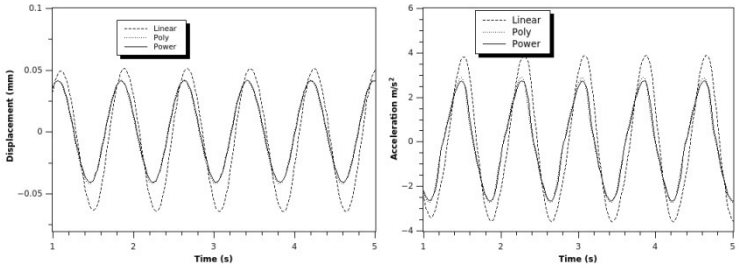

(a) (b)

Fig. 10 Steady state response of the sprung mass subjected to a sine wave road disturbance (a) displacement and (b) acceleration

The steady state acceleration response of the sprung mass can be observed in fadlyimage10b.jpg where again the peak-to-peak amplitude of the linear model is larger than the polynomial and power model. The larger peak-to-peak amplitude of the linear model shows that the damping coefficient value is smaller compared to the nonlinear models.

Another observation that can be seen from the graph is the phase shift of the response between the linear model and the nonlinear model. This phase shift occurs because of the different damping coefficient values between these models with the linear model having a larger coefficient compared to the nonlinear models. Since the shift is almost similar for the polynomial and power models thus it can be concluded that the damping coefficients of these two models are equal at this speed and frequency.

VII. CONCLUSIONS

A commercially available damper was tested on an MTS damper testing system and its characteristic was obtained. The important characteristic of the damper is the force-velocity relationship since the damping force is a

function of velocity. From the data obtained through experiment three types of damper models were developed through curve fitting method. The models are linear model, polynomial model and power model. From the value of the RMS error and the force validation figure it can be concluded that the nonlinear models could represent the actual characteristic more accurately compared to the linear model. Based on the simulations of the quarter car model linear damping model produces higher displacement overshoots and longer settling period while the nonlinear damper showed smaller overshoot and shorter settling period. Thus, the level of accuracy of linear damping models might be a good representation of an actual automotive damper.

VIII. ACKNOWLEDGEMENT

The authors acknowledge the financial support of the Ministry of Education Malaysia under research grant ERGS12-032-0032 and PRGS12-009-0009 and PROTON Bhd. for supporting in conducting the experiment of the shock absorber.

REFERENCES

Dixon, J.C., 2007. The shock absorber handbook. West Susex: John Wiley & Sons. Ltd.

Duym, S., Steins, R. and Reybrouock, K., 1997. Evaluation of shock absorber models. *Vehicle System Dynamics*, 27(2), pp. 109-127.

Dzierżek, S., Knapczyk, M., & Maniowski, M., 2008. Extending passive pampers functionality for specific ride and handling requirements. Czasopismo Techniczne. Mechanika, 105(6-M), pp. 39-47.

Ferdek U., and Łuczko J., 2012. Modeling and analysis of a twin-tube hydraulic shock absorber. *Journal of Theoretical and Applied Mechanics*, 50(2), pp. 627-638.

Gillespie, T.D., 1992. Fundamentals of Vehicle Dynamics. Pensylvania: Society of Automotive Engineers, Inc.

Ihsan, S. I., Ahmadian, M., Faris, W. F., & Blancard, E. D. (2009). Ride performance analysis of half-car model for semi-active system using RMS as performance criteria. Shock and Vibration, 16(6), 593-605.

Kasteel, R. V., Cheng-Guo, W., Lixin, Q., Jin-Zhao, L., & Guo-Hong, Y., 2005. A new shock absorber model for use in vehicle dynamics studies. *Vehicle system dynamics*, 43(9), 613-631.

Lee, K., 1997. Numerical Modelling for the Hydraulic Performance Prediction of Automotive Monotube Dampers, *Vehicle System Dynamics,* 28, pp. 25-39.

Rao, M. D., Gruenberg, S., & Torab, H., 1999. Measurement of dynamic properties of automotive shock absorbers for NVH. *Society of Automotive Engineers*.

Subramanian, S., Surampudi, R., & Thomson, K. R., 2003. Development of a nonlinear shock absorber model for low-frequency nvh applications. *SAE SP*, pp. 79-84.

Surace, C., Worden, K., & Tomlinson, G. R. 1992. An improved nonlinear model for an automotive shock absorber. *Nonlinear Dynamics*, 3(6), pp. 413-429.

Zhu, J. J., Khajepour, A., Esmailzadeh, E., & Kasaiezadeh, A. 2012. Ride quality evaluation of a vehicle with a planar suspension system. *Vehicle System Dynamics*, 50(3), pp. 395-413.